

Assessment of future climate change impacts on snowmelt and stream water quality for a mountainous high-elevation watershed using SWAT

Saet Byul Kim · Hyung Jin Shin · Minji Park ·
Seong Joon Kim

Received: 29 August 2014/Revised: 21 November 2014/Accepted: 10 December 2014/Published online: 21 December 2014
© The International Society of Paddy and Water Environment Engineering and Springer Japan 2014

Abstract The Soil and Water Assessment Tool model was applied to assess the potential climate change impact on snowmelt and the non-point source pollution discharges in a 6,640.0 km² high-elevation watershed of South Korea. For the snowmelt parameters of the model, Terra Moderate Resolution Imaging Spectroradiometer image was used to obtain the snow cover depletion curve. The model was calibrated using 11 years of data from 2000 to 2010 that included daily runoff and monthly sediment, total nitrogen (TN), and total phosphorus (TP). The climate change impacts on snowmelt in the watershed were evaluated for Special Report on Emission Scenarios A2, A1B, and B1, scenarios (HadCM3) and Representative Concentration Pathway (RCP) 4.5 and 8.5 scenarios (HadGEM3-RA). With the temperature increase of 4.33 °C during the snowmelt period in 2080s (2060–2099) RCP 8.5 scenario based on baseline period (1981–2010), the future snowmelt decreased to 39.9 % during snowmelt period (November–April). Turning the reduced snowmelt discharges into rain-runoff discharges under the 45.7 % increase of precipitation caused increase of future sediment, TN, and TP loads

to 53.0, 118.2, and 137.5 % respectively. The future increases of TN and TP loads can stimulate the algal bloom and the eutrophication of the dam reservoir.

Keywords Snowmelt · Snow depletion curve · Stream water quality · Climate change · SWAT

Introduction

It is widely accepted that although seasonal snow cover forms only a small fraction of world's fresh water, its hydrologic contribution is significant. In high and mid-latitudes, runoff from shallow snow cover often provides 80 percent or more of the annual surface runoff (Maidment 1993). In Korea, the snowmelt by winter snowfalls contributes considerably to water resources in high-altitude regions. For example, the frequency of heavy snowfall event (>20 cm in depth) is often greater than 40 % of the total events in mid-eastern mountainous areas, and the snowmelt from these regions supplies a considerable amount of stream discharge during spring period. However, a quantitative analysis of watershed snowmelt is generally difficult to perform because of the insufficient spatial snow information and complexity of the physical processes involved with snowmelt and runoff generations (Shin et al. 2007).

As climate change appearance has affected recent patterns in frequency, strength, spatial range, and duration of snowfall, the snowmelt changes will provoke various problems in hydrology and water quality. For example, as the snow decreases in the Rocky mountains of American west, river stages become lower and policy decisions related to spring water resources were questioned (Stewart et al. 2005; Regonda et al. 2005). Moreover, while snowfall

S. B. Kim
Water Environment Research Department, National Institute of
Environmental Research, Incheon, Korea

H. J. Shin
K-water Institute, Daejeon, Korea

M. Park
Han River Environmental Research Center, Gyeonggi-Do, Korea

S. J. Kim (✉)
Department of Civil and Environmental System Engineering,
Konkuk University, Seoul, Korea
e-mail: kimsj@konkuk.ac.kr

of deep drifts during the winter melt in early spring, the forest fire frequency and strength increase (Westerling et al. 2006). In the context of assessing the impacts of climate change on water resources, it is important to adequately evaluate the impacts of climate change on snowmelt and the subsequent flow changes.

Recently, many studies have evaluated the effects of climate change on the hydrology of snowmelt-driven watersheds. Vicuna et al. (2010) showed climate change impacts on the hydrology of a snowmelt-driven basin in Chile. Tahir et al. (2010) simulated snowmelt runoff under various climate scenarios in a large mountainous watershed in Northern Pakistan by employing the snowmelt runoff model (SRM), which is based on a simple degree–day method for snowmelt simulation. Kobierska et al. (2011) investigated the climate change effects on snowmelt discharge of a glacierized watershed. In the study, two different models including a detailed energy balance model and a conceptual runoff model were used to compare the benefit of each model for snowmelt simulation.

Many models that deal with snowmelt and snow accumulation have been developed (Martinec 1960; Anderson 1968, 1976; Rango and Martinec 1979; Blöschl and Kirnbauer 1991; Jordan 1991; Coughlan and Running 1997; Fontaine et al. 2002; Garen and Marks 2005). Soil and Water Assessment Tool (SWAT) is one of the many models that include snow processes with simulation of

water balances. It was initially developed for comprehensive modeling of the impacts of management practices on water yield, sediment yield, crop growth, and agricultural chemical yields in large ungauged basins (Arnold et al. 1998).

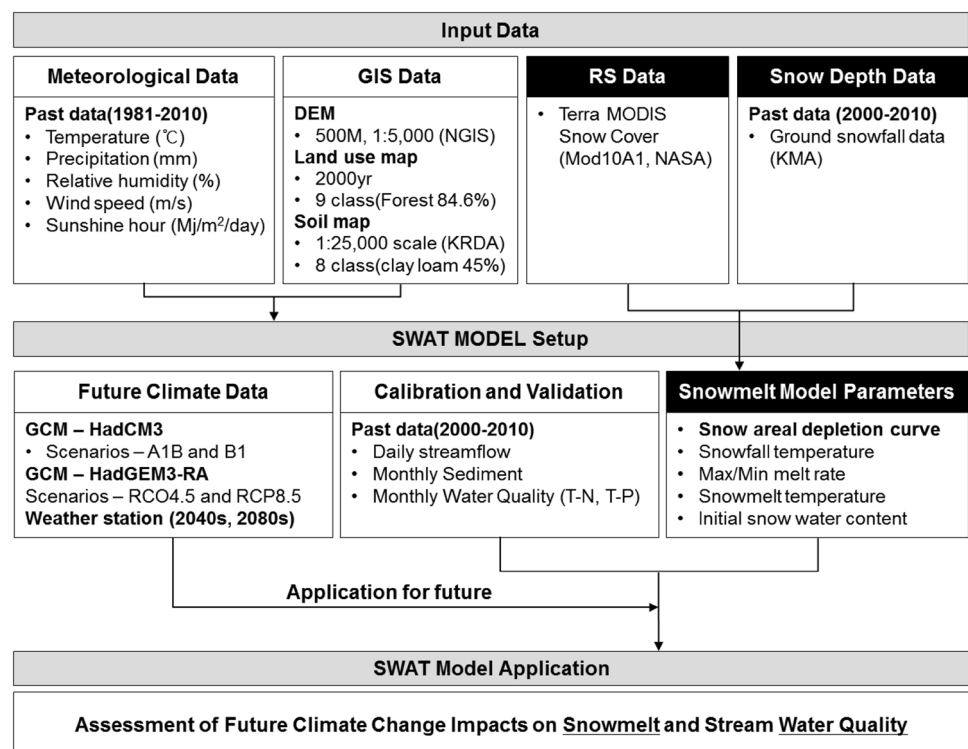
This study is to assess the impact of potential climate change on snowmelt and its non-point source pollution loads to stream in a 6,640 km² high-elevation watershed using SWAT model. The Terra MODIS (moderate resolution imaging spectroradiometer) image is used to obtain the snow cover area (SCA) and determine the snow depletion parameters using 11-year (2000–2010) data. After the SWAT model is set up using the observed dam inflow, sediment, TN, and TP data, the model is applied to evaluate the future climate change impact on the snowmelt runoff and the nutrients load to the dam reservoir under five scenarios (HadCM3 SRES A2, A1B, and B1 and HadGEM3-RA RCP4.5 and 8.5). Figure 1 shows the schematic flow chart of this study.

Data and method

Study area

A 6,640 km² mountainous watershed was selected. It is located in the north-eastern part of South Korea within the latitude–

Fig. 1 Schematic flow chart of the study process



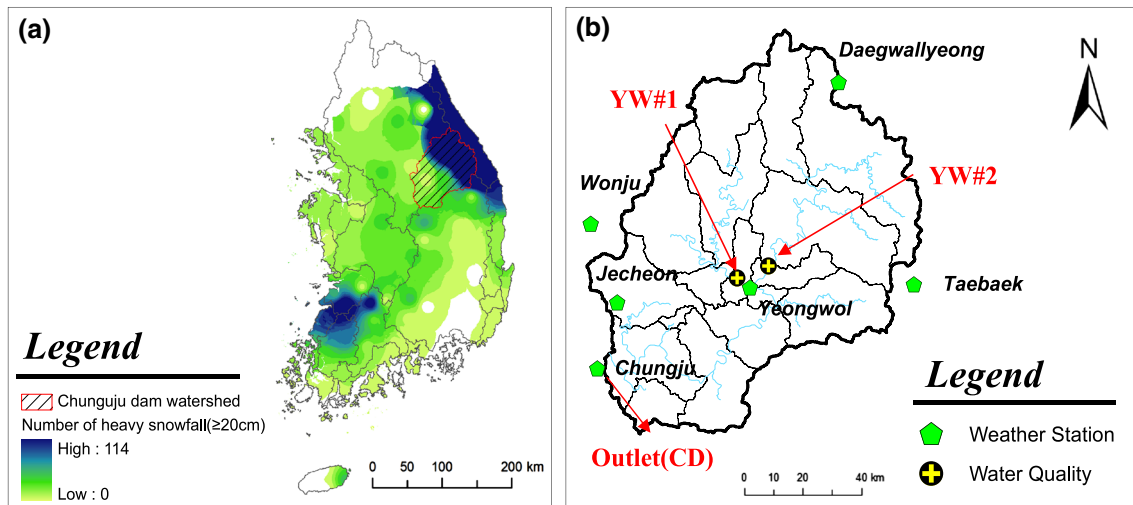


Fig. 2 The study area: **a** heavy snowfall area of South Korea and **b** Chungju dam study watershed

longitude range of 127.9°E–129.0°E, 36.8°N–37.8°N. The watershed is one of the heavy snowfall areas in South Korea. Figure 2a shows the snowfall area in South Korea with the heavy snowfall frequency over 20 cm during 30 years (1981–2010). The study watershed is marked with slashed lines, and Fig. 2b shows the enlarged study watershed with the subwatershed boundaries for modeling and the locations of weather and gaging stations. The watershed elevation ranges from 112 to 1,562 m, with average slope of 36.9 %. The annual average precipitation is 1,261 mm, and the mean temperature is 9.4 °C over the last 30 years (1981–2010). For model calibration, 10-year (2000–2010) data at six weather stations, three stream water level gaging stations (YW #1, YW #2, and CD), and two stream water quality measuring stations (YW #1 and YW #2) were used.

SWAT snow hydrology description

The SWAT model, developed by Arnold et al. (1998), is a physically based continuous, long-term, distributed parameter model designed to predict the impact of land management practices on hydrology, snowmelt, sediment, and agricultural chemical yields in large watersheds with varying soils, land use, and management conditions over long periods of time (Srinivasan and Arnold 1994; Rosenthal et al. 1995; Arnold et al. 1998, 1999).

In the SWAT model, snowmelt hydrology is realized on an hydrologic response unit (HRU) basis. The model has the function of snow mass routing and areal depletion estimation. Depending on data availability and modeling accuracy, one sub-basin may have one or several HRUs. When the daily mean air temperature is below a defined value, the precipitation within an HRU is classified as snow and the liquid water equivalent of snow precipitation is

added to snowpack. The snowpack increases with additional snowfall but decreases by snowmelt or sublimation. The mass balance for the snow pack on a daily basis is

$$SNO = SNO + R_{day} - E_{sub} - SNO_{melt}, \tag{1}$$

where *SNO* is the water content of snow pack (mm), *R_{day}* is the amount of precipitation (mm), *E_{sub}* is the amount of sublimation (mm), and *SNO_{melt}* is the amount of snowmelt (mm).

The amount of snow is expressed as depth over the total HRU area. The factors that contribute to variable snow coverage are usually similar across years, making it possible to correlate the areal coverage of snow with the amount of snow present in the sub-basin at a given time.

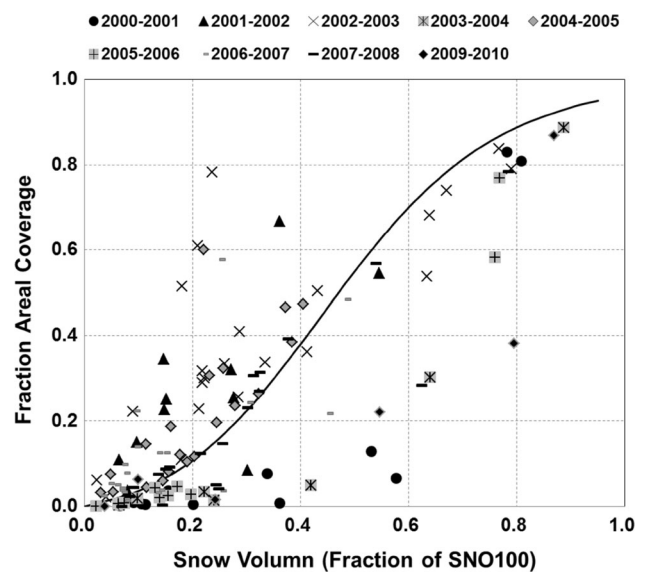


Fig. 3 Snow depletion curves (2000–2010) derived from Terra MODIS images

Table 1 Snow depletion curve shape factor (2000–2010) derived from Terra MODIS images

Dataset	cov ₁	cov ₂	SNO50COV
2000–2001	7.03	10.56	0.70
2001–2002	0.60	3.78	0.40
2002–2003	0.18	4.39	0.45
2003–2004	7.03	10.56	0.70
2004–2005	0.82	4.02	0.42
2005–2006	7.03	10.56	0.70
2006–2007	1.18	4.39	0.45
2007–2008	1.58	4.81	0.48
2009–2010	7.03	10.56	0.70
Average	3.61	7.07	0.56

SNO50COV fraction of *SNOCOVMX* that provides 50 % cover, *cov₁* and *cov₂* values for determining the shape of snow depletion curve

This correlation is expressed as an areal depletion curve, which is used to describe the seasonal growth and recession of the snow pack as a function of the amount of snow present in the sub-basin (Anderson 1976).

The areal depletion curve requires a threshold depth of snow, *SNO*₁₀₀, to be defined above which there will always be 100 % cover. The threshold depth is unique to the watershed depending on factors such as vegetation distribution, wind loading of snow, wind scouring of snow, interception, and aspect. The equation for the curve based on a natural logarithm can be expressed as

$$sno_{cov} = \frac{SNO}{SNO_{100}} \cdot \left(\frac{SNO}{SNO_{100}} + \exp\left(\text{cov}_1 - \text{cov}_2 \cdot \frac{SNO}{SNO_{100}}\right) \right)^{-1}, \quad (2)$$

where *sno_{cov}* is the fraction of the HRU area covered by snow, *SNO* is the water content of the snow pack on a given day (mm), *SNO*₁₀₀ is the threshold depth of snow at 100 % coverage (mm), and *cov*₁ and *cov*₂ are coefficients that define the shape of the curve. The values used for *cov*₁ and *cov*₂ are determined by solving the equation and using two known points: 95 % coverage at 95 % *SNO*₁₀₀ and 50 % coverage (*SNO*_{50COV}) at a user-specified fraction of *SNO*₁₀₀. As the value for *SNO*₁₀₀ increases, the influence of the areal depletion curve will assume more importance in snowmelt processes.

Snow coverage from Terra MODIS NDSI (Normalized Difference Snow Index)

To obtain the SCA by HRU base in study watershed, Terra MODIS image was used. MODIS is an imaging spectroradiometer to provide imagery of the Earth's surface and clouds in 36 spectral bands from 0.4 to 14.0 μm (Barnes

Table 2 Changes in annual and snowmelt periods precipitation and temperature with the five climate change scenarios

Period	Scenarios	PCP variation (%)	TMN difference (°C)	TMX difference (°C)
AP	HadCM3 A1B			
	2040s	5.8	0.63	2.26
	2080s	8.0	1.86	3.51
	HadCM3 B1			
	2040s	7.6	1.45	3.11
	2080s	10.1	2.32	4.00
	HadCM3 A2			
	2040s	5.3	0.59	2.25
	2080s	8.2	2.10	3.79
	HadGEM3 RCP4.5			
	2040s	−6.0	1.40	1.11
	2080s	2.4	2.43	2.04
SP	HadCM3 RCP8.5			
	2040s	−5.3	1.98	1.66
	2080s	15.2	4.65	4.30
	HadCM3 A1B			
	2040s	4.4	0.16	1.79
	2080s	−6.6	1.31	3.10
	HadCM3 B1			
	2040s	11.8	1.04	2.64
	2080s	−5.8	2.23	3.84
	HadCM3 A2			
	2040s	3.7	0.25	1.85
	2080s	−13.5	1.65	3.26
SP	HadGEM3 RCP4.5			
	2040s	9.2	1.43	0.83
	2080s	32.0	2.30	1.64
	HadGEM3 RCP8.5			
	2040s	0.6	1.84	1.19
	2080s	45.7	4.64	4.02

PCP precipitation, *TMN* minimum temperature, *TMX* maximum temperature, *AP* annual period (November–October), *SP* snowmelt period (November–April)

et al. 1998). The MODIS/Terra Snow Cover 1-Day L3 Global 500m Grid (MOD10A1) for 10 years from 2000 to 2010 during the snow season (November–April) was used in this study. The data were developed using MODIS bands 4 (0.545–0.565 μm) and 6 (1.628–1.652 μm) by calculating the normalized difference snow index (NDSI) (Hall et al. 1995):

$$\text{NDSI} = (\text{band 4} - \text{band 6}) / (\text{band 4} + \text{band 6}). \quad (3)$$

Meanwhile, the distribution maps by snow depth during the snow period are necessary to determine the snow depletion parameters of Eq. (2) for the watershed. Thus, a set of snow depth distributions (SDD) in time series was

Table 3 The calibrated SWAT model parameters at three stations

Parameter	Definition	LB	UB	Adjusted value		
				YW #1	YW #2	CD
Hydrology						
ALPHA_BF	Baseflow alpha factor (days)	0	1	0.35	0.50	0.30
CH_N	Manning coefficient for channel	0.01	0.3	0.01	0.01	0.01
CH_K2	Effective hydraulic cond. of main channel	−0.01	150	50	70	70
CN2	Curve number adjustment ratio	−20 %	+20 %	9	2	9
ESCO	Soil evaporation compensation	0	1	0.8	0.8	0.4
GW_DELAY	Groundwater delay time (days)	0	500	120	110	110
SOL_AWC	Available water capacity	−20 %	+20 %	5	–	–
Snowmelt						
SFTMP	Snowfall temperature	0	5	2		
SMTMP	Snowmelt base temperature	0	5	1.5		
SNOCOVMX	Min. snow water content that corresponds to 100 % snow cover	0	500	1		
SNO50COV	Fraction of SNOCOVMX that provides 50 % cover	0	1	Each (Table 1)		
TIMP	Snowpack temp. lag factor	0	1	1		
SMFMX	Max. snowmelt factor	0	10	4.5		
SMFMN	Min. snowmelt factor	0	10	4.5		
Parameter	Definition	LB	UB	Adjusted value		
				YW #1	YW #2	YW #2
Water quality						
SS						
SPCON	Channel re-entrained linear parameter	0.0001	0.01	0.0002	0.0001	
SPEXP	Channel re-entrained exponent parameter	1	2	1	1	
PRF	Peak rate adjustment factor for sediment routing in main channel	0	2	1	0.02	
LAT_SED	Sediment concentration in lateral flow	0	5000	0	10	
USLE_P	USLE P factor	0	1	0.005	0.02	
CH_COV	Channel cover factor	−0.001	1	0.7	0.8	
CH_EROD	Channel erodibility factor	−0.05	0.6	0.04	0.02	
BIOMIX	Biological mixing efficiency	0	1	0.7	0.01	
T-N						
SOL_OrgN	Initial organic nitrogen concentration in the soil layer	0	100	1	0.01	
T-P						
PSP	Phosphorus availability index	0.01	0.7	0.69	0.01	
GWSOLP	Soluble phosphorus concentration	0	1000	0.0001	0	
SOL_ORGP	Initial organic phosphorus concentration in soil layer	0	100	100	0	

LB lower bound, UB upper bound

made from the inverse distance weight (IDW) interpolated map using the six ground snowfall data by masking it with the MODIS SCA map. As in Eq. (2), the areal snow depletion curve requires the threshold depth of snow, SNO_{100} and the coefficients cov_1 and cov_2 . By analyzing the SNO_{100} and the corresponding SCA, and the fractions from the SDD set of each year, the snow depletion curve was determined as shown in Fig. 3. Table 1 shows the derived parameters for snow depletion curve of each year (2000–2010). The key parameter SNO50COV for determining the depletion shape, the 50 % coverage at a fraction

of SNO_{100} ranged from 0.42 to 0.70. This means that the watershed main snowfall area usually covers 42–70 % at high elevation of the watershed as seen in Fig. 2a and the snow is depleted as time passes. The average SNO50COV for nine datasets was 0.56. The average value of the parameters was applied for future snow cover depletion.

Climate change scenarios

The Intergovernmental Panel on Climate Change (IPCC) published future scenarios in its Special Report on

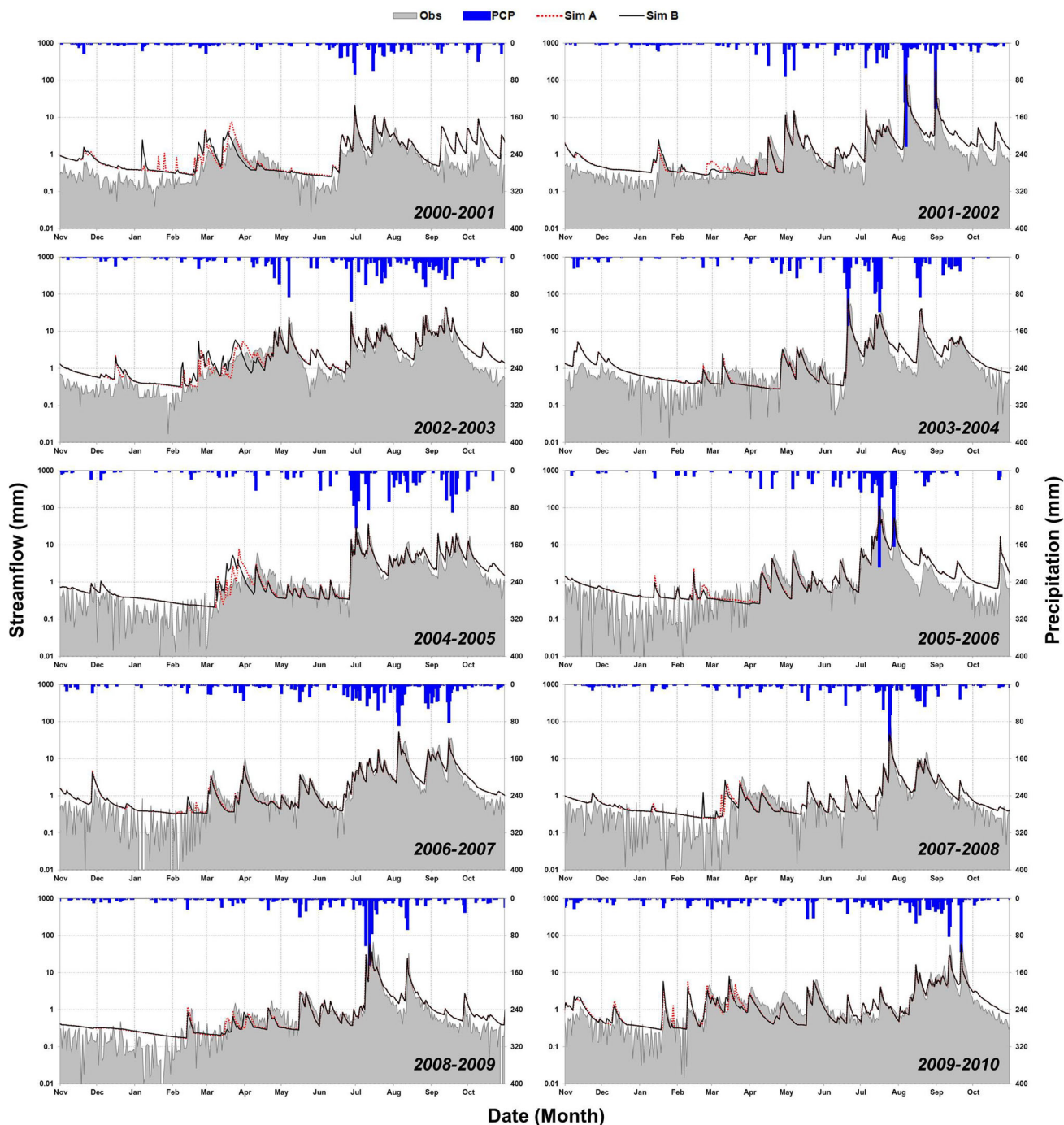


Fig. 4 Hydrograph comparison between observed and simulated discharges by varying snowmelt parameters of each year (Sim A) and fixing parameters (Sim B) at CD (2000–2010) location

Emissions Scenarios (SRES) document (Nakicenovic 2000). Among all SRES scenarios, four marker scenarios (A1, A2, B1, and B2) are commonly used (Van Vuuren and O'Neill 2006). The A1 and B1 scenarios emphasize ongoing globalization and project future worlds with fewer differences between regions, whereas the A2 and B2 scenarios emphasize regional and local social, economic, and environmental development and project more

differences (IPCC 2007). The three A1 groups are distinguished by their technological emphasis: fossil intensive (A1FI), non-fossil energy sources (A1T), or a balance across all sources (A1B). In this study, the SRES A1B, A2, and B1 scenarios of HadCM3 by the Hadley Centre at UK Meteorological Office (HC-UKMO) were used since Korea Meteorological Administration (KMA) has cooperated with HC-UKMO. The future data

Table 4 Summary of the SWAT model calibration and validation statistics for daily runoff with and without snowmelt parameters during the snowmelt period at CD location

Year (Nov–Apr)	Snow depth (cm)	P (mm)		Q (mm)			SM (mm)		NSE		R ²	
		Obs.	Sim.	Obs.	Sim.A	Sim.B	Sim.A	Sim.B	Sim.A	Sim.B	Sim.A	Sim.B
2000–2001	128.6	170.2	172.5	90.7	87.5	81.3	100.7	18.1	0.44	0.43	0.10	0.03
2001–2002	56.5	257.0	248.5	83.5	100.6	96.0	35.4	27.2	0.71	0.75	0.61	0.66
2002–2003	129.7	354.3	373.8	191.6	163.8	149.8	66.8	30.1	0.26	0.19	0.72	0.70
2003–2004	59.6	230.0	231.8	100.5	89.1	85.7	52.1	42.5	0.64	0.67	0.26	0.29
2004–2005	86.9	213.4	187.7	101.3	81.3	78.5	53.7	7.3	0.33	0.28	0.60	0.54
2005–2006	52.2	177.0	187.1	105.0	91.4	85.6	38.1	33.1	0.50	0.50	0.75	0.67
2006–2007	49.7	262.9	242.4	131.3	139.9	135.9	20.8	6.7	0.56	0.50	0.83	0.82
2007–2008	80.5	189.4	155.5	82.6	69.5	67.2	39.8	19.6	0.69	0.64	0.58	0.48
2008–2009	33.1	196.1	137.2	55.3	63.2	64.6	25.8	20.3	0.81	0.80	0.50	0.47
2009–2010	92.5	372.5	330.6	181.4	156.4	146.2	52.6	34.9	0.35	0.23	0.47	0.38
Mean	76.9	242.3	226.7	112.3	104.3	99.1	48.6	24.0	0.53	0.50	0.54	0.51

P precipitation, Q runoff, SM snowmelt, NSE Nash–Sutcliffe model efficiency, R² determination coefficient, Sim. A with snowmelt parameters, Sim. B without snowmelt parameters

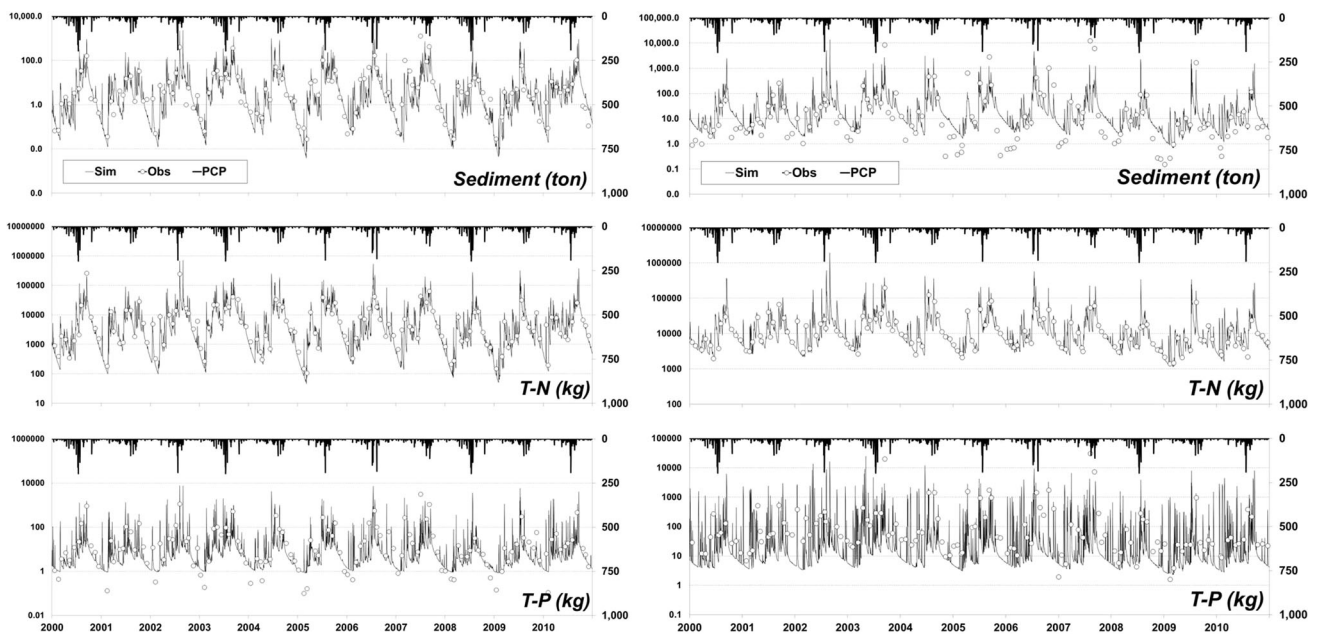


Fig. 5 Comparison between observed and simulated stream water quality at YW #1 (left) and YW #2 (right) stations

(2011–2100) of 96 km × 73 km grid size were spatially corrected to ensure that the observed data (1981–2010, baseline) and the scenario of the same period have similar statistical properties by the methods of Alcamo et al. (1997) among various statistical transformations. The monthly data to daily generation were downscaled using the LARS-WG downscaling method. LARS-WG is a stochastic weather generator which can be used for the

simulation of weather data at a single site (Racsko et al. 1991), under both current and future climate conditions. Details for the downscaling process are found in Park et al. (2011).

Recently, the IPCC (2013) has published new climate change scenarios based on Representative Concentration Pathways (RCPs) with a possible range of radiative forcing values in 2100. The RCP 2.6 scenario is characterized by

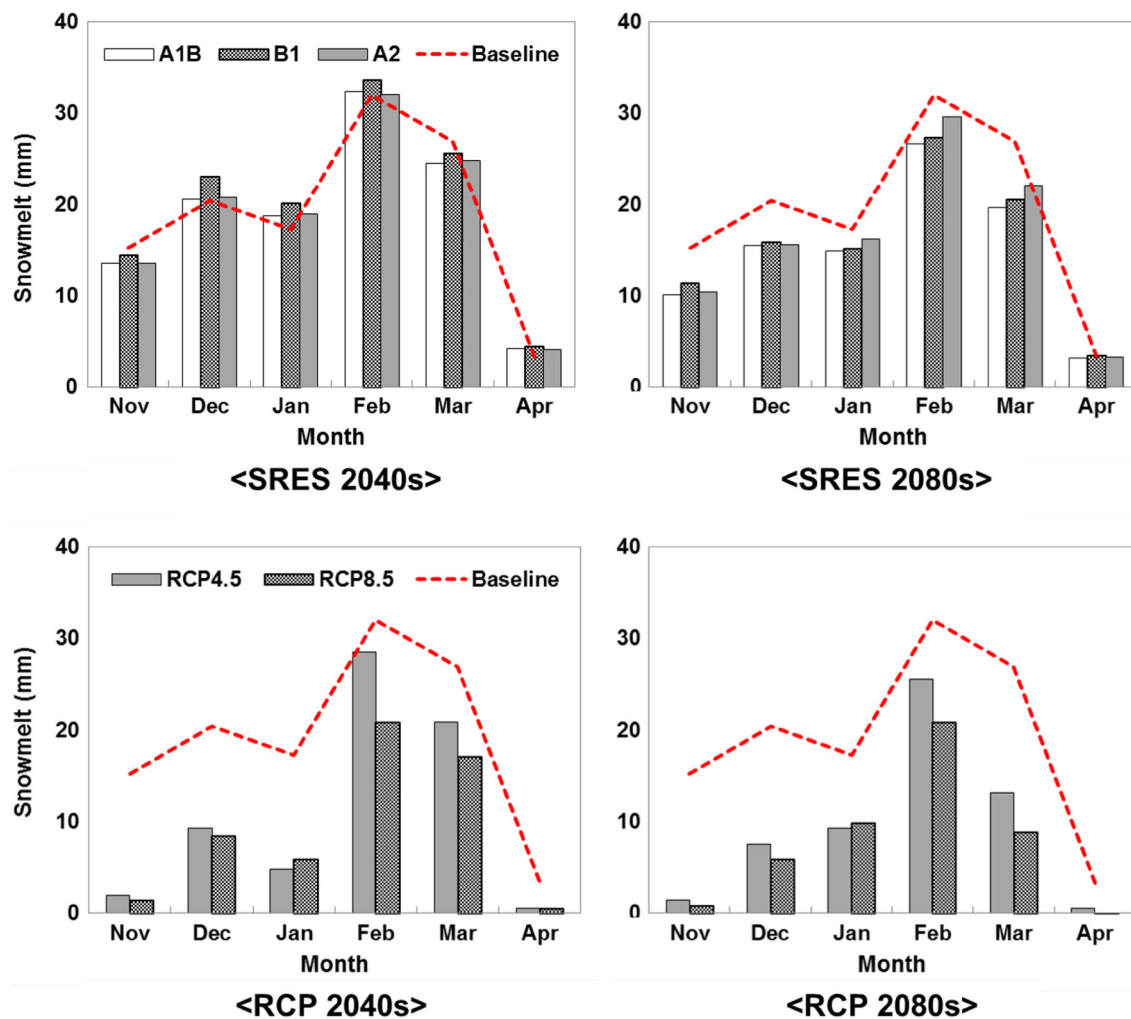


Fig. 6 The effects of climate change on monthly snowmelt from two SRES (*top*) and RCPs (*bottom*) climate change scenarios

very low greenhouse gas concentrations, producing forcings around 3.1 W/m^2 mid-century, and dropping to 2.6 W/m^2 by 2100. In order to achieve such radiative forcing levels, greenhouse gas concentrations are reduced substantially over time. The RCP4.5 (medium low) and RCP 6.0 (medium high) are stabilization scenarios on the assumption that technologies and strategies for reducing greenhouse gas emissions are stabilized, where the total radiative forcing levels is stabilized before 2100 and after 2100 by employing a range of technologies and strategies for reducing greenhouse gas emissions. The RCP8.5 is characterized by high greenhouse gas concentration levels, stabilizing emissions post-2100 and atmospheric concentrations post-2200 (Moss et al. 2010). In this study, RCP4.5 and RCP8.5 scenarios of HadGEM3-RA were used. HadGEM3-RA is a regional atmospheric model based on the atmospheric component of HadGEM3, the latest model developed by HC-UKMO. The KMA regenerated the

scenarios with $12.5 \text{ km} \times 12.5 \text{ km}$ resolution using the dynamic downscaling method.

For the five scenarios (HadCM3 SRES A1B, HadCM3 SRES A2, HadCM3 SRES B1, HadGEM3-RA RCP4.5, and HadGEM3-RA RCP8.5), the future changes of climate variables were arranged for the 2040s (2020–2059) and 2080s (2060–2099) using the baseline (1981–2010).

Table 2 summarizes the results of statistical analysis for the trends of average precipitation and temperature in annual and snowmelt period (November–April) for the five scenarios. The biggest changes in temperature and precipitation were $+4.64 \text{ }^\circ\text{C}$ at minimum temperature and $+45.7 \%$ in 2080s snowmelt period under HadGEM3 RCP8.5 scenario. The future precipitation and temperature of RCPs (AR5) showed bigger changes than those of SRES (AR4). This result may come from the temporal and spatial resolutions between AR4 (monthly, $2.5^\circ \times 3.75^\circ$) and AR5

Table 5 Summary of the future predicted annual and snowmelt period runoff ratio and snowmelt ratio for the five climate change scenarios

Scenario	Period	<i>P</i> (mm)	<i>Q</i> (mm)	<i>QR</i> (%)	<i>SM</i> (mm)	<i>SMR</i> (%)
Baseline (1981–2010)	AP	1,305.4	767.6	58.8	115.1	8.8 (43.6)
	SP	264.0	110.5	41.9	115.1	
HadCM3						
A1B						
2040s	AP	1,380.5	846.5	61.3	114.3	8.3 (41.3)
	SP	275.7	110.7	40.2	113.9	
2080s	AP	1,409.6	879.2	62.4	89.7	6.4 (36.4)
	SP	246.6	82.8	33.6	89.7	
HadCM3						
B1						
2040s	AP	1,404.7	868.1	61.8	121.6	8.7 (41.0)
	SP	295.1	128.2	43.4	121.1	
2080s	AP	1,436.7	902.9	62.8	121.6	8.5 (37.5)
	SP	248.8	85.3	34.3	93.4	
HadCM3						
A2						
2040s	AP	1,374.2	840.4	61.2	114.6	8.3 (41.7)
	SP	273.9	109.6	40.0	114.2	
2080s	AP	1,413.0	882.4	62.4	97.1	6.9 (42.5)
	SP	228.3	74.6	32.7	97.1	
HadGEM3-RA						
RCP4.5						
2040s	AP	1,227.3	449.9	36.7	65.8	5.4 (22.8)
	SP	288.4	61.4	21.3	65.8	
2080s	AP	1,336.2	521.8	39.0	57.4	4.3 (16.5)
	SP	348.4	108.4	31.1	57.4	
HadGEM3-RA						
RCP8.5						
2040s	AP	1,236.6	536.3	43.4	53.8	4.4 (20.3)
	SP	265.5	63.9	24.1	53.8	
2080s	AP	1,220.8	437.8	35.9	45.9	3.8 (11.9)
	SP	384.6	102.9	26.8	45.9	

P precipitation, *Q* runoff, *QR* runoff ratio (=Q/P), *SM* snowmelt, *SMR* snowmelt ratio (=SM/P), *AP* annual period (November–October), *SP* snowmelt period (November–April)

(daily, $0.125^\circ \times 0.125^\circ$). The averaged characteristics at coarse resolution may be resolved to represent the spatial variation at finer resolution.

Results and discussion

SWAT model calibration and validation

The SWAT model was calibrated for 10 years (2000–2010) of daily runoff data at three locations (YW #1, YW #2, and CD) and monthly stream water quality (SS, TN, and TP)

data at two locations (YW #1 and YW #2). Table 3 shows the calibrated parameters for hydrology, snowmelt, and stream water quality. The snow parameters, SFTMP and SMTMP were referenced by analyzing the temperatures of snowfall and rainfall days.

With the help of SNO50COV value fixed for each year, the other snow parameters were calibrated. Figure 4 shows the observed versus simulated runoff using the SNO50COV value (Sim A) of each year and fixing SNO50COV with 0.56 (Sim B) at CD station (2000–2010). As seen in Fig. 4, the runoff from melting snow is detected to increase in March and April. Table 4 summarizes the statistical

Table 6 Percentage changes of SS, TN, and TP loads in annual and snowmelt periods with the five climate change scenarios

Scenario	SS (%)		TN (%)		TP (%)	
	AP	SP	AP	SP	AP	SP
SRES						
HadCM3						
A1B						
2040s	-29.8	-43.0	-1.0	-11.2	17.3	9.3
2080s	-24.5	-46.4	-6.2	-10.7	8.9	-2.4
B1						
2040s	-18.2	-26.4	7.9	4.1	30.7	31.1
2080s	-24.7	-25.5	0.5	-0.4	21.3	-15.7
A2						
2040s	-8.9	-12.5	-8.9	-15.4	-13.3	-20.8
2080s	-12.7	-13.2	-11.6	-16.6	-16.7	-20.3
RCP						
HadGEM3-RA						
4.5						
2040s	-24.1	-16.9	47.4	98.1	95.2	152.6
2080s	-13.8	15.7	63.6	120.1	115.0	171.4
8.5						
2040s	4.1	44.4	64.5	145.2	114.0	225.7
2080s	19.9	53.0	69.6	118.2	110.8	137.5

results for the SWAT-simulated snowmelt (SM) and runoff (Q) during the snowmelt period (November–April), respectively. The 10-year average Nash–Sutcliffe model efficiency (NSE) for the snowmelt period was 0.53 (Sim A) and 0.50 (Sim B), respectively. The runoff considering snowmelt parameter SNO50COV in each year was simulated well compared to the results of fixing the parameter and the NSE was enhanced by 0.03. Although the snowmelt is a function of many variables, the relatively low NSE value during the snowmelt period in SWAT modeling may come from the uncertainty of SDD generated by six ground snowfall data, snow water equivalent (SWE) by wet or dry snowpack, and the air temperature (cool or warm) for the snowmelt.

Figure 5 shows the calibration and validation results for water quality at YW #1, YW #2 with snowmelt parameters. The NSE for SS, TN, and TP during the calibration and validation periods were 0.72, 0.54, and 0.70 at YW #1, and 0.75, 0.85, and 0.70 at YW #2, respectively. The coefficients of determination (R^2) for SS, TN, and TP were 0.87, 0.74, and 0.85 at YW #1, and 0.61, 0.88, and 0.62 at YW #2, respectively. Other detailed discussion for parameter sensitivity and model results of the study watershed can be found in Park et al. (2011).

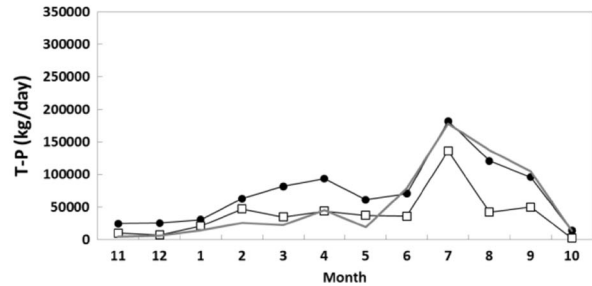
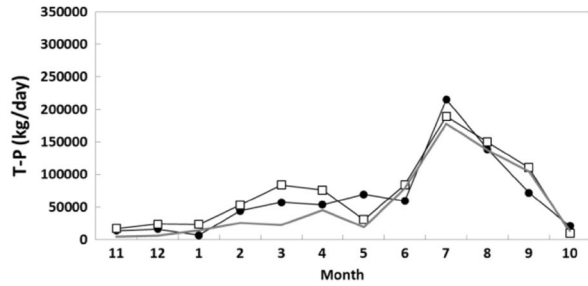
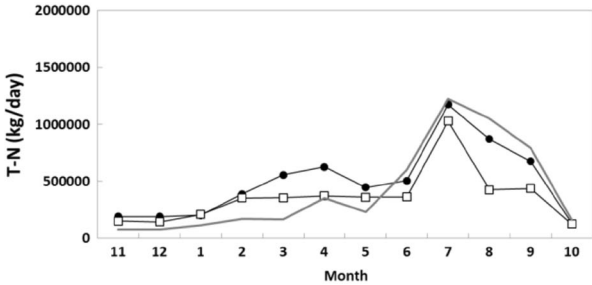
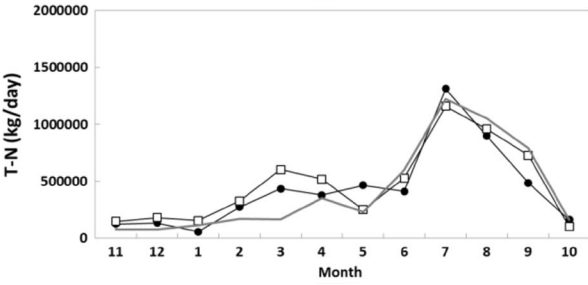
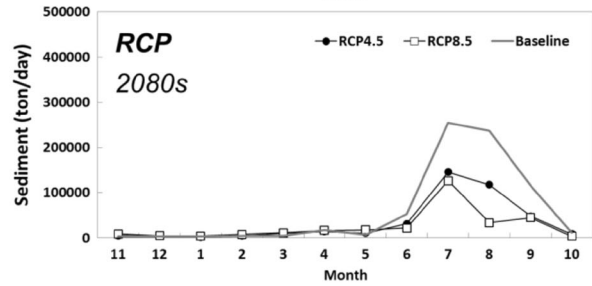
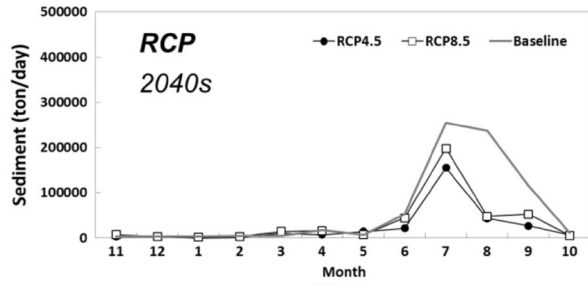
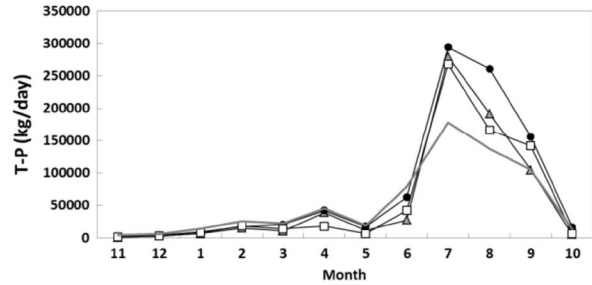
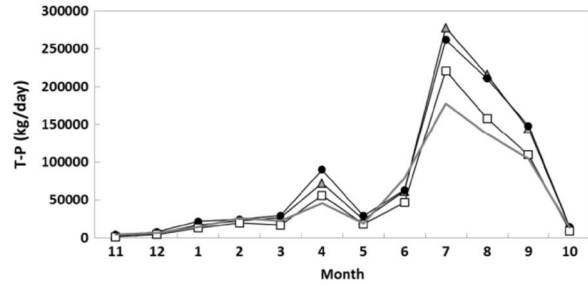
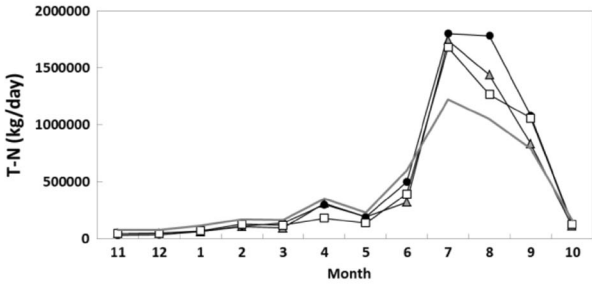
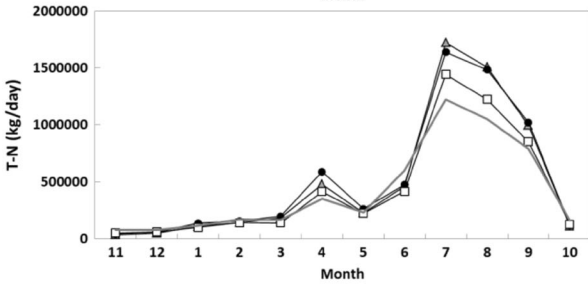
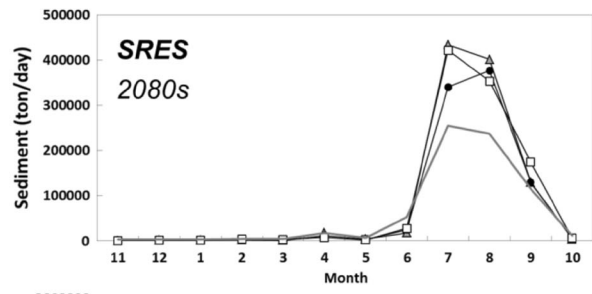
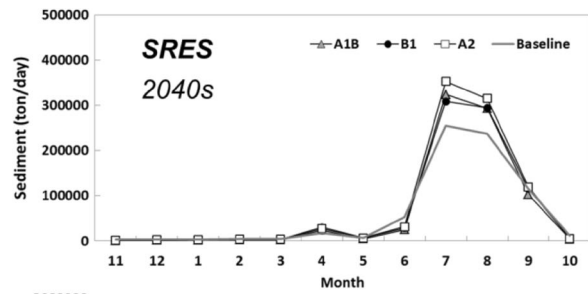
Fig. 7 The changes of 2040s and 2080s monthly sediment load, TN, and TP by SRES and RCP climate change scenarios

The future climate change impact on snow hydrology and stream water quality

Using the SWAT calibrated parameters in Table 3 and the average values of SNO50COV, cov_1 , and cov_2 in Table 1, the five future climate change scenarios were applied to the study watershed. Figure 6 shows the future 2040s and 2080s monthly snowmelt for the five climate change scenarios. The future snowmelt amount decreased for all scenarios as it goes to 2080s compared to baseline. Meanwhile, the future snowmelt during the melt period decreased largely for the two RCP scenarios than the three SRES scenarios. This may come from the big increase of future minimum temperature in RCP scenarios as seen in Table 3. The future temperature condition turned the snowfall to rainfall and increased the 3-month overall water yields not by melt flow but by rain runoff from November to January.

Table 5 summarizes the future snowmelt and the runoff during the snowmelt period for the five climate change scenarios. Looking at the results of HadCM3 scenarios, the future runoff by snowmelt (SMR) showed similar values ranging from 37.5 to 42.5 % compared to the value of 43.6 % of the baseline period. Meanwhile, the results of HadGEM3-RA showed different patterns for the snowmelt-induced runoff. The future snowmelt decreased up to 45.9 mm (39.9 %) in 2080s HadGEM RCP8.5 scenario from 115.1 mm (100 %) in baseline period (1981–2010). For this scenario, the runoff discharge from November to April decreased by 15.1 from 41.9 % in baseline to 26.8 % in 2080s, while the 1-year whole discharge decreased by 22.9 from 58.8 % in baseline period to 35.9 % in 2080s. As mentioned above, the snowmelt ratio in 2080s HadGEM RCP8.5 scenario decreased up to 11.9 % on account of snowfall reduction by temperature rise during snowmelt period. Thus, the future runoff by rainfall from November to April becomes more important even when the amount is relatively low comparing with the remaining period runoff.

After the evaluation of future snow hydrology, the impact of future snowmelt change on stream water quality was evaluated in terms of SS, TN, and TP at the watershed outlet. Figure 7 shows the changes of future monthly SS, TN, and TP loads, and Table 6 summarizes the percent changes in future annual and snowmelt period for the five climate change scenarios. Looking at the results of the three SRES scenarios in Fig. 7, the future monthly SS, TN, and TP loads during the snowmelt period showed similar trends of big increase in April with the baseline loads. On



the other hand, the two RCP scenarios showed different trends of big increases in March for SS and from February for TN and TP.

As seen in Table 6, the future SS, TN, and TP loads during snowmelt period under RCP scenarios showed big increases in annual total, while the SRES scenarios showed overall decreases for the three loads. This was primarily caused by the big differences of precipitation during the snowmelt period between the RCP and SRES scenarios as listed in Table 2. In addition, due to the big differences of snowmelt between SRES and RCP scenarios as shown in Fig. 6, much more runoff discharges turned the snowmelt discharges into the rainfall-runoff contribution in RCP scenarios. The three SRES precipitation changes of -13.5% in 2080s B1 scenario to $+11.8\%$ in 2040s B1 scenario during the snowmelt period resulted in the changes of -46.4% in 2080s A1B scenario to -12.5% in 2040s A2 scenario for SS, -16.6% in 2080s A2 scenario to $+4.1\%$ in 2040s B1 scenario for TN, and -20.8% in 2040s A2 scenario to $+31.1\%$ in 2040s B1 scenario for TP, respectively, while the two RCP precipitation changes of $+0.57\%$ in 2040s RCP8.5 scenario to $+45.7\%$ in 2080s RCP8.5 scenario during the snowmelt period resulted in the changes of -16.9% in 2040s RCP4.5 scenario to $+53.0\%$ in 2080s RCP8.5 scenario for SS, $+98.1\%$ in 2040s RCP4.5 scenario to $+145.2\%$ in 2040s RCP8.5 scenario for TN, and $+137.5\%$ in 2080s RCP8.5 scenario to $+225.7\%$ in 2040s RCP8.5 scenario for TP, respectively. The future increases of sediment, TN, and TP loads flowed in the dam reservoir during the snowmelt period may contribute to the algal bloom in spring period with the nutrients rise by turnover of the water and the eutrophication problem for the long time progress under the condition of future temperature increase.

Summary and conclusions

This study evaluated the potential climate change impact on snowmelt and stream water quantity for a 6,640 km² high-elevation watershed in South Korea using SWAT model. To determine the SWAT snowmelt parameters, Terra MODIS images were used to obtain the SCA, and the SDD was developed using snowfall data of ground meteorological stations to determine the shape of snow cover depletion curve (SCDC) of the study watershed. For 10 datasets (2000–2010) during the snowmelt period (November–April), the SNO50COV parameter, that is, the 50 % coverage at a fraction of SCDC that determines the shape of snow depletion process, showed values of 0.42–0.70 and an average value of 0.56. Using the snow parameters of each year, the SWAT model was calibrated using daily runoff discharge data at three locations and

monthly stream water quality (SS, TN, and TP) data at two locations. The 10-year NSE for runoff was 0.54 during the snowmelt period. The snow on the ground is affected by the wind especially at high elevation, and the compaction and melting processes are certainly different by the terrain aspect with steep slopes. These two factors can improve the snow hydrology when incorporated in the snowmelt modeling process.

Using the SWAT calibrated parameters and the average value of SNO50COV, the five future climate change scenarios of were applied to the study watershed and the future projection results were arranged for the 2040s (2020–2059) and 2080s (2060–2099) using the baseline (1981–2010). Among the five tested scenarios, the future snowmelt decreased to 45.9 mm (39.9 %) in 2080s HadGEM RCP8.5 scenario from 115.1 mm (100 %) in baseline period. For the RCP scenarios, more discharges turned the snowmelt discharges into the rainfall-runoff contribution by the future temperature and precipitation increases during the snowmelt period. The 2 RCP precipitation changes of $+45.8$ to $+54.5\%$ during the snowmelt period resulted in the changes of -16.9 to $+53.0\%$ for SS, $+98.1$ to $+145.2\%$ for TN, and $+137.5$ to $+225.7\%$ for TP, respectively. The future increases of sediment, TN, and TP loads flowed in the dam reservoir during the snowmelt period may contribute to the algal bloom in spring period with the nutrients rise by turnover of the water and the eutrophication problem for the long time progress under the condition of future temperature increase. The examination of various climate change scenarios to high-elevation watershed hydrology is to be considered for the changes of winter snowfalls and the impacts on the spring snowmelt. Even though the results of this study give plausible clue for the future snowmelt impact on hydrologic water cycle and the stream water quality, there may be other factors that need to be considered to explain the impact by the future land-use change and the eco-hydrological changes like the changes of soil environment, leaf canopy inception of snowfall, and snowmelt mechanism considering the litter fall and humus soil layer.

Acknowledgments This research was supported by a grant (14AWMP-B079364-01) from Water Management Research Program funded by Ministry of Land, Infrastructure and Transport of Korean government.

References

- Alcamo J, Döll P, Kaspar F, Siebert S (1997) Global change and global scenarios of water use and availability: an application of WaterGAP 1.0. Center for Environmental Systems Research (CESR), University of Kassel, Kassel
- Anderson EA (1968) Development and testing of snow pack energy balance equations. *Water Resour Res* 4(1):19–37

- Anderson EA (1976) A point of energy and mass balance model of snow cover. NOAA Tech. Rep. NWS, vol 19, pp 1–150
- Arnold JG, Srinivasan R, Muttiyah RS, Williams JR (1998) Large area hydrologic modeling and assessment, part I: model development. *JAWRA J Am Water Resour Assoc* 34(1):73–89
- Arnold JG, Srinivasan R, Muttiyah RS, Allen PM (1999) Continental scale simulation of the hydrologic balance. *JAWRA J Am Water Resour Assoc* 35(5):1037–1051
- Barnes WL, Pagano TS, Salomonson VV (1998) Pre-launch characteristics of the moderate resolution imaging spectroradiometer (MODIS) on EOS-AM1. *IEEE Trans Geosci Remote Sens* 36(4):1088–1100
- Blöschl G, Kirnbauer R (1991) Point snowmelt models with different degrees of complexity—internal processes. *J Hydrol* 129(1):127–147
- Coughlan JC, Running SW (1997) Regional ecosystem simulation: a general model for simulating snow accumulation and melt in mountainous terrain. *Landsch Ecol* 12(3):119–136
- Fontaine TA, Cruickshank TS, Arnold JG, Hotchkiss RH (2002) Development of a snowfall–snowmelt routine for mountainous terrain for the soil water assessment tool (SWAT). *J Hydrol* 262(1):209–223
- Garen DC, Marks D (2005) Spatially distributed energy balance snowmelt modelling in a mountainous river basin: estimation of meteorological inputs and verification of model results. *J Hydrol* 315(1):126–153
- Hall DK, Riggs GA, Salomonson VV (1995) Development of methods for mapping global snow cover using moderate resolution imaging spectroradiometer data. *Remote Sens Environ* 54(2):127–140
- IPCC (2007) *Climate Change 2007: the physical science basis*, IPCC Contribution of Working Group I to the Fourth Assessment Report of the Intergovernmental Panel on Climate Change. Cambridge University Press, Cambridge
- IPCC (2013) *Climate Change 2013: the physical science basis*, IPCC Contribution of Working Group I to the Fifth Assessment Report of the Intergovernmental Panel on Climate Change. Cambridge University Press, Cambridge
- Jordan RE (1991) A one-dimensional temperature model for a snow cover. Technical documentation for SNTherm.89. Cold Regions Research and Engineering Lab, Hanover
- Kobierska F, Jonas T, Magnusson J, Zappa M, Bavay M, Bosshard T, Paul F, Bernasconi SM (2011) Climate change effects on snow melt and discharge of a partly glacierized watershed in Central Switzerland (SoilTrec Critical Zone Observatory). *Appl Geochim* 26:60–62
- Maidment DR (1993) *Developing a spatially distributed unit hydrograph by using GIS*. IAHS Publication, Wallingford, p 181
- Martinez J (1960) The degree-day factor for snowmelt runoff forecasting, vol 51. IAHS Commission of Surface Waters, Wallingford, pp 468–477
- Moss RH, Edmonds JA, Hibbard KA, Manning MR, Rose SK, van Vuuren DP, Carter TR, Emori S, Kainuma M, Kram T, Meehl GA, Mitchell JFB, Nakicenovic N, Riahi K, Smith SJ, Stouffer RJ, Thomson AM, Weyant JP, Wilbanks TJ (2010) The next generation of scenarios for climate change research and assessment. *Nature* 463:747–756
- Nakicenovic N et al (2000) Special report on emissions scenarios: a special report of Working Group III of the Intergovernmental Panel on Climate Change (No. PNNL-SA-39650). Pacific Northwest National Laboratory/Environmental Molecular Sciences Laboratory, Richland/USA
- Park JY, Park MJ, Ahn SR, Park GA, Yi JE, Kim GS, Srinivasan R, Kim SJ (2011) Assessment of future climate change impacts on water quantity and quality for a mountainous dam watershed using SWAT. *Trans ASABE* 54(5):1725–1737
- Racsko P, Szeidl L, Semenov M (1991) A serial approach to local stochastic weather models. *Ecol Model* 57(1):27–41
- Rango A, Martinec J (1979) Application of a snowmelt-runoff model using Landsat data. *Nord Hydrol* 10(4):225–238
- Regonda SK, Rajagopalan B, Clark M, Pitlick J (2005) Seasonal cycle shifts in hydroclimatology over the western United States. *J Clim* 18(2):372–384
- Rosenthal WD, Srinivasan R, Arnold JG (1995) Alternative river management using a linked GIS-hydrology model. *Trans ASAE* 38(3):783–790
- Shin HJ, Park GA, Kim SJ (2007) Tracing March 2004 and December 2005 heavy snowfall of South Korea using NOAA-AVHRR images. *J Korean Soc Agric Eng* 49(3):33–40
- Srinivasan R, Arnold JG (1994) Integration of a basin-scale water quality model with GIS. *JAWRA J Am Water Resour Assoc* 30(3):453–462
- Stewart IT, Cayan DR, Dettinger MD (2005) Changes toward earlier streamflow timing across western North America. *J Clim* 18:1136–1155
- Tahir R, Ellis PR, Butterworth PJ (2010) The relation of physical properties of native starch granules to the kinetics of amylolysis catalysed by porcine pancreatic α -amylase. *Carbohydr Polym* 81(1):57–62
- Van Vuuren DP, O'Neill BC (2006) The consistency of IPCC's SRES scenarios to 1990–2000 trends and recent projections. *Clim Change* 75(1–2):9–46
- Vicuna S, Dracup JA, Lund JR, Dale LL, Maurer EP (2010) Basin-scale water system operations with uncertain future climate conditions: methodology and case studies. *Water Resour Res* 46:W04505. doi:10.1029/2009WR007838
- Westerling AL, Hidalgo HG, Cayan DR, Swetnam TW (2006) Warming and earlier spring increase western US forest wildfire activity. *Science* 313:940–943